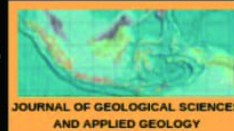


ISSN : 2579 - 3136

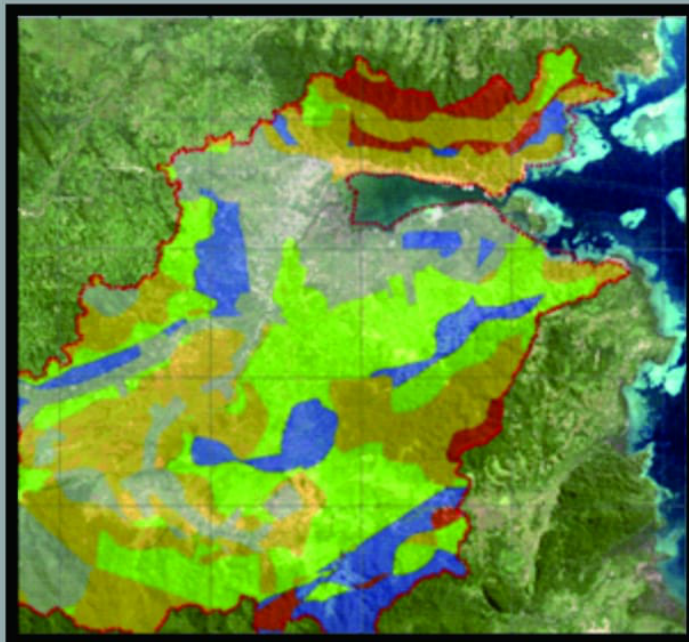
**JOURNAL OF GEOLOGICAL SCIENCES AND APPLIED GEOLOGY**



FACULTY OF GEOLOGICAL ENGINEERING  
UNIVERSITAS PADJADJARAN



VOL. 4 No. 2 AUGUST 2020



\*Due to the COVID-19 pandemic, this edition was published late on February 13, 2021

**PUBLISHED THREE TIMES A YEAR**

**PUBLISHED BY:**

**FACULTY OF GEOLOGICAL ENGINEERING  
UNIVERSITAS PADJADJARAN**

[OPEN JOURNAL SYSTEMS](#)

[JADWAL PENERBITAN](#)

[PANDUAN PENGGUNAAN](#)

[BERIKUTNYA DITANYAKAN](#)

**BERGUNA**

[Daftar Pengguna](#)

[Sandi](#)

[Lihat Saya](#)

[Login](#)

[PAuS Login](#)

**VERIFIKASI**

[t](#)

[gganan](#)

**IASA**

[isa Indonesia](#)

[Ubah](#)

**FEED**

**ARIAN**

[Kunci...](#)

[Jata :](#)

[ua](#)

[Cari](#)

[ri](#)

[Dasarkan Terbitan](#)

[Dasarkan Penulis](#)

[Dasarkan Judul](#)

[al Lain](#)

[egori](#)

**URAN HURUF**

[A](#) [A](#)

**ORMASI**

[uk Pembaca](#)

[uk Penulis](#)

[uk Pustakawan](#)

## Editor

Abdul Wahid Asykarulloh, Indonesia  
Nanda Natasia, Indonesia  
Muhammad Kurniawan Alfadli, Fakultas Teknik Geologi Universitas Padjadjaran, Indonesia  
ARIEF IRMANSYAH, Indonesia  
ERICK ERICK SANJAYA, Fakultas Teknik Geologi - Universitas Padjadjaran, Indonesia  
arfi Kurnia Arfiansyah, Teknik Geologi Universitas Padjadjaran, Indonesia  
Nur Khoirullah, Departement of Applied Geology, Faculty of Geological Engineering, Universitas Padjadjaran, Indonesia  
PRADNYA PARAMARTA RADITYA RENDRA, Universitas Padjadjaran, Indonesia

[OPEN JOURNAL SYSTEMS](#)

[JADWAL PENERBITAN](#)

[PANDUAN PENGGUNAAN](#)

[SERING DITANYAKAN](#)

### PENGGUNA

Nama Pengguna

Kata Sandi

Ingat Saya

Login

PAuS Login

### NOTIFIKASI

- [Lihat](#)
- [Langganan](#)

### BAHASA

Bahasa Indonesia ▾

Ubah

### RSS-FEED

#### PENCARIAN

Kata Kunci...

pada data :

Semua ▾

Cari

#### Telusuri

- [Berdasarkan Terbitan](#)
- [Berdasarkan Penulis](#)
- [Berdasarkan Judul](#)
- [Jurnal Lain](#)
- [Kategori](#)



### UKURAN HURUF



### INFORMASI

- [Untuk Pembaca](#)
- [Untuk Penulis](#)
- [Untuk Pustakawan](#)


[Beranda](#) > [Arsip](#) > [Vol 4, No 3 \(2020\)](#)

## Journal of Geological Science and Applied Geology

### Daftar Isi


#### Artikel

**THE SUSTAINABLE MANAGEMENT OF POST-MINING LANDUSE; AN AHP APPROACH A CASE STUDY: EX-SAND MINING IN INDRAMAYU REGENCY, WEST JAVA**

 *Ahmad Helman Hamdani, Johanes Hutabarat, Faisal Muhamadsyah*



**QUANTITATIVE GEOMORPHOLOGY EXPRESSION OF GEOLOGICAL STRUCTURES USING SATELLITE IMAGERY AND GEOSPATIAL ANALYSIS: AN EXAMPLE IN THE SOUTHERN PART OF MERAPI MOUNT, YOGYAKARTA, INDONESIA**

 *Herry Riswandi, Emi Sukiyah, Dina Tania*




**Geophysical Approach And Geochemistry Correlated To Discover Underground Water Flow Indicator To Mud Volcano In Quarter Volcanic System**

 *Pandji Ridwan, Kurnia Arfiansyah Fachrudin, Aldrin Ramadian, Kemala Wijayanti*



**THE APPLICATION OF LANDSAT IMAGERY PROCESSING FOR EROSION STUDY**

 *Emi Sukiyah, Kurnia Arfiansyah Fachrudin*



[OPEN JOURNAL SYSTEMS](#)

[JADWAL PENERBITAN](#)

[PANDUAN PENGGUNAAN](#)

[SERING DITANYAKAN](#)

#### PENGGUNA

Nama Pengguna

Kata Sandi

Ingat Saya

[Login](#)


[PAuS Login](#)

#### NOTIFIKASI

[Lihat](#)

[Langganan](#)

#### BAHASA

Bahasa Indonesia 

[Ubah](#)

#### RSS-FEED

#### PENCARIAN

Kata Kunci...

pada data :

Semua 

[Cari](#)

#### Telusuri

[Berdasarkan Terbitan](#)

[Berdasarkan Penulis](#)

[Berdasarkan Judul](#)

[Jurnal Lain](#)

[Kategori](#)



#### UKURAN HURUF



#### INFORMASI

[Untuk Pembaca](#)

[Untuk Penulis](#)

[Untuk Pustakawan](#)

## QUANTITATIVE GEOMORPHOLOGY EXPRESSION OF GEOLOGICAL STRUCTURES USING SATELLITE IMAGERY AND GEOSPATIAL ANALYSIS: AN EXAMPLE IN THE SOUTHERN PART OF MERAPI MOUNT, YOGYAKARTA, INDONESIA

Herry Riswandi<sup>1</sup>, Emi Sukiyah<sup>2</sup>, and Dina Tania<sup>3</sup>

<sup>1</sup>Department of Geology, Universitas Pembangunan Nasional Veteran Yogyakarta, 55283, Indonesia

<sup>2</sup>Department of Geological Sciences, Universitas Padjadjaran, Bandung 45363, Indonesia

<sup>3</sup>Department of Geology, Institut Sains & Teknologi Akprind Yogyakarta 55222, Indonesia

Corresponding Author : [herry.riswandi@upnyk.ac.id](mailto:herry.riswandi@upnyk.ac.id)

### ABSTRACT

*Research using morphotectonics parameters from a 30-m digital elevation model to evaluate satellite imagery data. It process by contour, slope, aspect, and hillshade analysis of geographic information system tools. For geological lineaments, drainage patterns and their relation with geological structures. Data analyzed in digital format reveals the lineament identifies 116 segments in north-south and east-west polar direction, with length from 0.2 to 4.6 km. Quantitative geomorphology is based on the slope and valley dimension in four watersheds to recognize recent tectonic activity located on the southern slopes. Digital quantitative geomorphic analyzed volcanic slope area to generate data along with the tectonic evolution in annual eruption. Furthermore, the results become references for recent tectonic activity on the volcanic slopes, with several exceptional values of the four watersheds. That indices of bifurcation ratio, drainage density (3.44-4.76), sinuosity of mountain front (3-4), valley floor width to valley height ratio (0.021-0.32), asymmetry factor (16.7-2), streams length gradient index (5.9-12.2), hypsometric (h/H 0.4-0.6 and a/A 0.4-0.5), transverse topography symmetry (0.47-0.87), elongation of basin ratio (0.003). The analyzed data results that structures are shifting. The geomorphological index can support tectonic activity assessment through the deformation of land from various volcanic deposits, uplift rate, and asymmetric river maturity.*

**Keywords:** morphotectonic, digital elevation model, geographic information system, volcanic, tectonic activity

### 1. INTRODUCTION

Tectonic plate activity on the Earth's surface can affect the landscape of geological structure, and land formation can determine morphotectonic characteristics. Several indexes assess the tectonic activity by quantifying different morphotectonic excellent indices (Doornkamp, 1986; Keller & Pinter, 1996; Bull & McFadden, 1977). Certain geological conditions will show the ability of land from the quantitative analysis reflected in the characteristics of landforms, including river dimensions, flow patterns, morphological alignment, flow density, and river basin ratio (Sukiyah et al., 2015; Omar M.A. Radaideh, 2016; Pike & Wilson, 1971). The form of quaternary volcanic land resulting from the volcano's morphological forms influence by tectonic activity and can see from the morphology of the river basin and its texture (Bali et al., 2016; Ahmed & Rao, 2016). The tectonic activity reflects the presence and dimension of earthquake, fractures, fold, and fault and can recognize

from the recorded evidence of unique slope aspect hillshade patterns in 30-m DEM. The evaluation of DEM from extracting satellite imagery needs calculations and hydrological modeling (Ganas et al., 2005; Shi & Xue, 2016; Yasin et al., 2016; Kaplay et al., 2016; Jing et al., 2014).

The watershed network is used as a digital modeling parameter to predict surface and subsurface water flows evolution associated with the neotectonic activity. Statistically, DEM characteristic can observe in ridge pattern with slope distribution, slope-aspect-hillshade dimension, and relation with rock outcrop. The color aspect in satellite imagery shown structural indicator polar lineaments (Moore et al., 1991; Szekely and Karátson, 2004; Wolosiewicz, 2016; Petrik & Jordan, 2017; Anfasha et al., 2016). Morphotectonic analyzed nine indices from DEM extraction: the ratio of bifurcation (Rb), drainage density (Dd), sinuosity of mountain front (Smf), Valley floor width to valley height ratio (Vf), asymmetry factor (AF), streams length gradient index (SL), hypsometric integral

(Hi), transverse topography symmetry (T), and elongation of basin ratio (Eb). The results processed data efficiently with an integrated and orderly workflow (Sharma et al., 2017; Helbig et al., 2017; Flores-Prieto et al., 2015; Bahrami, 2013). Moreover, all the computed geomorphic indices correlated with hydrological analysis on surface water flows (Hunter et al., 2015; McGuire et al., 2016). The analysis depicted in diagram models and geographic maps contained explicit map information as the evaluation source

(Napieralski et al., 2013; Çöltekin et al., 2016).

The location study area is on the southern slope of Merapi Mount in the upper reaches of the Gendol River, Opak River, Kuning River, and Boyong River, with dominated dendritic drainage pattern. Located between latitudes 110° 22' 00 – 110° 29' 30 N, and longitudes 7° 35' 0 – 7° 46' 30 E, and it has a total catchment area of 244 km<sup>2</sup> (Figure 1).

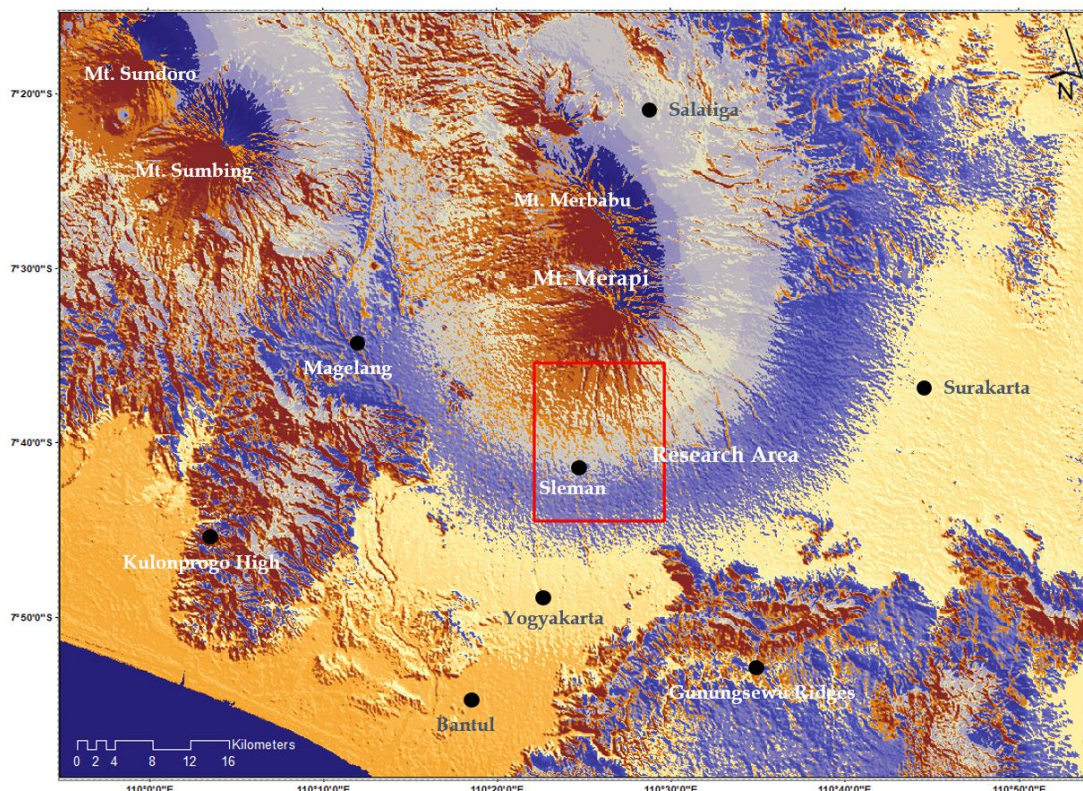


Figure 1. The research location is in the Sleman Regency, north of Yogyakarta City, with research object in the red box is observing the pattern of Gendol River, Opak River, Kuning River, and Boyong River. Map using SRTM 1 Arc-Second Global 30-m DEM with raster assigning a color to each unique value.

## 2. GEOLOGY

Merapi Mt. is composed of Quaternary rock formations (Paripurno, 2009; Charbonnier et al., 2013), composed of Young Merapi volcano deposits composed of tuff, ash, breccias, agglomerates, lava, deposits of avalanches (Gertisser et al., 2012). Old Merapi volcano deposits compose of breccia, agglomerates, andesite lava, and olivine basalt. Merapi Mt. locates between Northern Serayu Mountains with Southern Serayu Mountains, separated by young volcanic deposits from Merapi. Merapi Mt. place in the center of the depression zone in Central Java

and grow in the middle of a joint point between the lineament of volcanic Ungaran–Telomoyo–Merbabu–Merapi and Lawu–Merapi–Sumbing–Sindoro–Slamet. Also, Mt. Merapi, located in the significant meeting fault of Semarang, directed North-South, and Solo Fault directed West-East (Bemmelen, 1949). Merapi volcanic activity from 1961 to 1994 directed tend to West and Southwest, but in 1994 Merapi debris flow start to change direction to the South in the upper stream of Boyong River (Paripurno, 2009). In 2006, the pyroclastic flow changed direction to the southeast the upstream of the Gendol river (Figure 2).

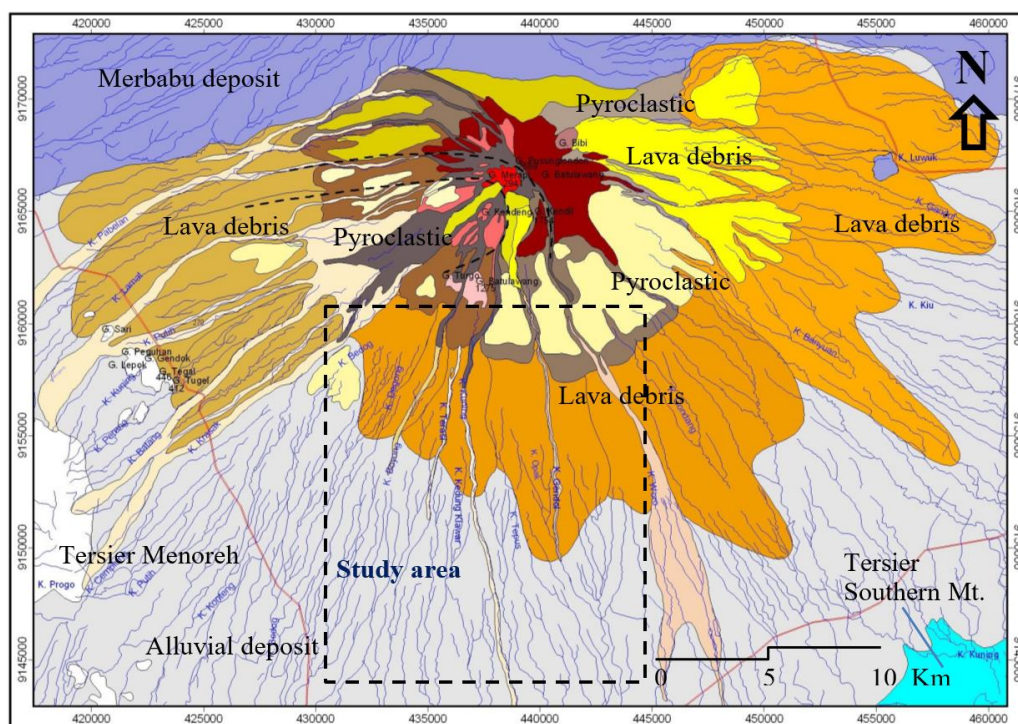


Figure 2. Geology and structural of Merapi Mount composed of lava debris, pyroclastic, and alluvial deposit (Paripurno, 2009).

### 3. METHODS

The analysis process uses a simple grid method to simplify calculations. The analyzed data will be converted to digital DEM data to process on the GIS, which use to analyze surface data in the form of elevation, slope, aspect, and hillshade. Morphometry measure calculates the quantitative variables of surface formation used to determine the value of the geomorphic index and tectonic activity level. Measurement includes dimensional aspects, river segment azimuth, aligned azimuth, flow density, river order, river ratios, elevation, and slope (Keller & Pinter, 1996). Measurements at Gendol River, Opak River, Kuning River, and Boyong River, and data generated from each river calculated to find morphotectonic values, using DEM data to determine morphology and river alignment. Using spatial imagery is analyzed on Quater deposits that show landforms, lithology, and river flow.

A score of the existing geomorphic index using each variable's formula, and then used to analyze tectonic activity. Bifurcation of the ratio (Rb) is the result of the comparison of the number of a specific order ( $\sum n$ ) river segments with the number of next order ( $n+1$ ) river segments (Verstappen, 1983).

$$Rb = \frac{\sum n}{n+1} \quad (1)$$

Drainage density (Dd) obtain by calculating the total streamflow length compared to the total watershed area (Strahler, 1957).

$$Dd = \frac{\sum Ls}{A} \quad (2)$$

The mountain front (Smf) sinuosity results from comparing the mountain's surface length long straight of the mountain face (Doornkamp, 1986).

$$Smf = \frac{Lmf}{Ls} \quad (3)$$

Valley ratio or comparison of valve width and height (Vf) obtain by comparing alley width with the height of the right and left valleys and the valley ratio elevation (Bull & McFadden, 1977).

$$Vf = \frac{2Vfw}{[(Eld-Esc)+(Erd-Esc)]} \quad (4)$$

Asymmetry factor or the value of river asymmetry (AF) can show the tectonic effect seen from the flow pattern (Molin et al., 2004; Kaplay et al., 2016). It can obtain by comparing the river basin area with the total area of the river basin (Keller & Pinter, 1996).

$$AF = 100 \times \frac{Ar}{At} \quad (5)$$

The river gradient index (SL)'s stream length or values rives from the river's total length multiplication. The elevation difference ratio

from the point calculates by the river's length (Keller & Pinter, 1996).

$$SL = \frac{\Delta H}{\Delta L} \times L \quad (6)$$

Hypsometric integrals (Hi) calculate the average elevation difference with minimum elevation, divided by the maximum elevation difference with minimum elevation (Pike & Wilson, 1971).

$$Hi = \frac{H_{mean} - H_{min}}{H_{max} - H_{min}} \quad (7)$$

Transverse topographic symmetry (T) calculates from the midline distance ratio from the valley to the maximum height with the diameter spacing from the valley to the minimum height (Cox, 1994; Keller & Pinter, 1996).

$$T = \frac{Da}{Dd} \quad (8)$$

Elongation of basin ratio (Eb) is obtaining from the ratio of roots to diameter of the river basin's circle, divided by phi, with the watershed's length (Schumm, 1956; Molin et al., 2004).

$$Eb = \frac{2\sqrt{\frac{Ab}{\pi}}}{lb} \quad (9)$$

## 4. RESULT AND DISCUSSION

### 4.1 DEFORMATION

The shape of the stream can determine by comparing the established river pattern. The shape of the river that looks shaped like a bird feather extends from the north to the South. The shape shows the flooding area's characteristics are relatively smaller than other forms of river patterns—topographic analysis view as a 3D analysis applied to surface data. And for a general understanding of the direction, the shape of the river, and variations of landform. To determine the topographic landscape can be taken from analysis of surface data in elevation, slope, aspect, and hillshade. Elevation data extracted from DEM imagery processed by using GIS toolbox system. GIS toolbox system in the 3D analyst tools section on raster surface contour. The same extraction procedure results in raster surface slope, raster surface aspect, and raster surface hillshade (Table 1 and Figure 3). The elevation data using the WGS 1984 UTM Zone 49S coordinate system projection extracted an arc-second raster with a contour interval of 12.5 meters.

Table 1. Statistical percentage processing of percent slope, azimuth of slope (aspect), and topographic relief (hillshade).

Classification	Slope Values	Aspect Values	Hillshade Values
Count	12,936,578.0	12,936,578.0	129,221,178.0
Minimum	0	-1	0
Maximum	77.841	359.944	254.0
Sum	393,752,261.6	2,028,123,562.0	1,884,092,663.0
Mean	30.437	156.774	145.803
Standard Deviation	22.142	107.562	65.468

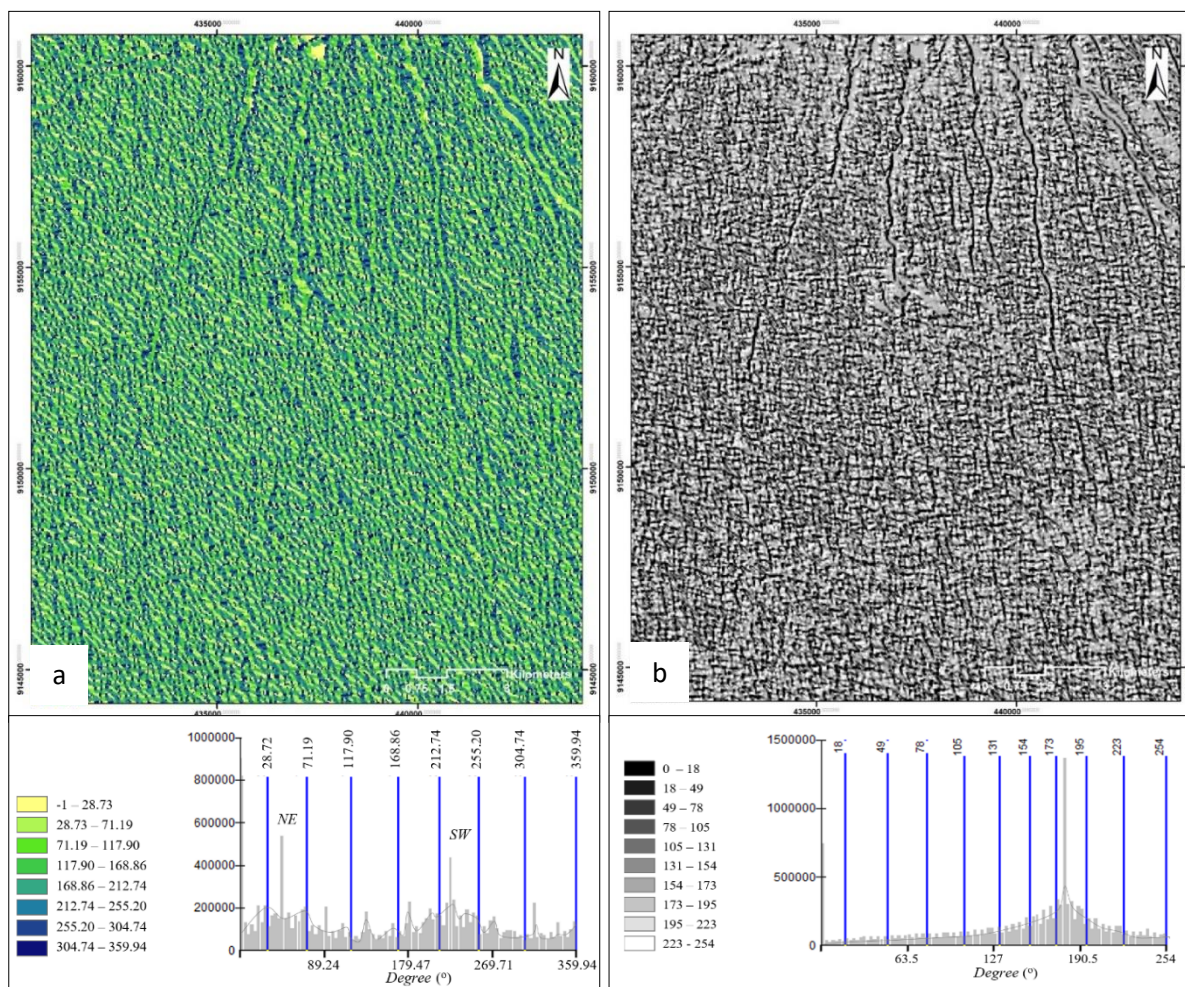


Figure 3. (a) The DEM data aspect processing is classified to show the inclination degree, thus showing the valley's flow and the ridge. The legend of the azimuth division of the slope on the raster surface aspect and the slope gradient graph on the map base on the DEM data. The classification of the slope direction is mostly towards the Northeast and Southwest. (b) Hillshade images to observe the straightness of streams and surface structures. The legend of topographical relief division on hillshade, and a graph of relief topography on a map based on DEM data with 45° sun height. Most slopes towards the East.

#### 4.2 LINEAMENTS OF STRUCTURE AND RIVER SEGMENT

DEM data processing use to determine the geological structure's alignment pattern and the straightness of the river segment,

review the morphological changes and the evolution of river curves in each watershed area in the rose diagram. The alignment of the structure and straightness of rivers shows a common direction (Figure 4).



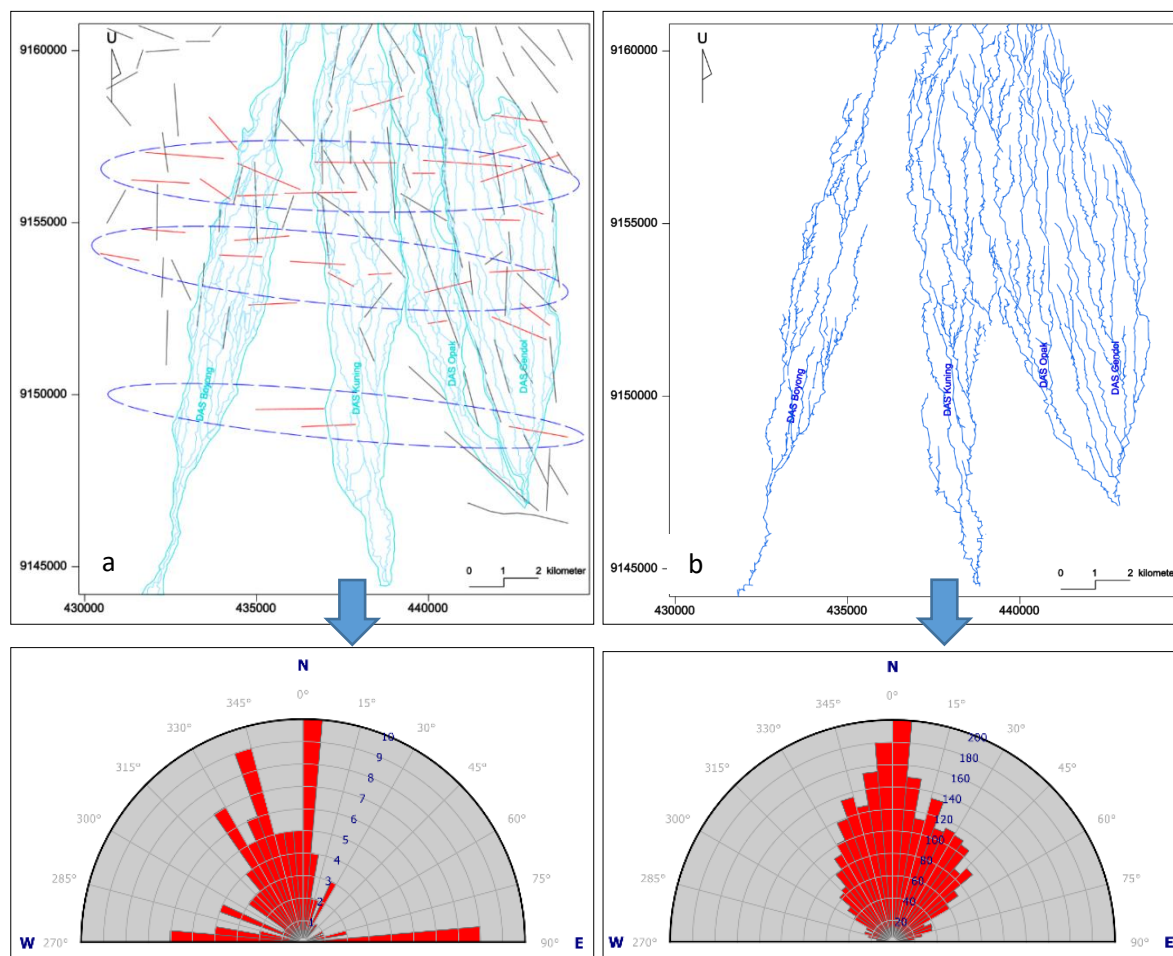


Figure 4. (a) Hillshade, slope, aspect, and contour of DEM process a drainage lineament map. (b) Hillshade, slope, aspect, and contour of DEM process a geological structure lineament map.

The mean ( $\bar{x}$ ) lineament direction straightness of the river divides into four quadrants of calculation, the first quadrant with angle  $0^{\circ}$ – $90^{\circ}$ , second quadrant with angle  $91^{\circ}$ – $180^{\circ}$ , third quadrant with angle  $181^{\circ}$ – $270^{\circ}$ , fourth quadrant with angle  $271^{\circ}$ – $359^{\circ}$ . The rose diagram of the

topography lineament figure that the  $\bar{x}$  of first quadrant direction  $N55.8^{\circ}E$ , the  $\bar{x}$  of second quadrant direction  $N139.5^{\circ}E$ , the  $\bar{x}$  of third quadrant  $N194.2^{\circ}E$ , and the  $\bar{x}$  of fourth quadrant  $N334.3^{\circ}E$  (Table 2 and Figure 5).

Table 2. Lineament direction calculation on each river with a rose diagram.

River	Lineament mean ( $\bar{x}$ ) direction			
	1 <sup>st</sup> quadrant	2 <sup>nd</sup> quadrant	3 <sup>rd</sup> quadrant	4 <sup>th</sup> quadrant
Gendol	N $23^{\circ}$ E	N $154^{\circ}$ E	N $204^{\circ}$ E	N $335.7^{\circ}$ E
Opak	N $27.4^{\circ}$ E	N $151.4^{\circ}$ E	N $206.3^{\circ}$ E	N $332^{\circ}$ E
Kuning	N $29.1^{\circ}$ E	N $152^{\circ}$ E	N $206^{\circ}$ E	N $332.7^{\circ}$ E
Boyong	N $31.1^{\circ}$ E	N $151.6^{\circ}$ E	N $201^{\circ}$ E	N $340^{\circ}$ E
Topography	N $55.8^{\circ}$ E	N $139.5^{\circ}$ E	N $194.2^{\circ}$ E	N $334.3^{\circ}$ E

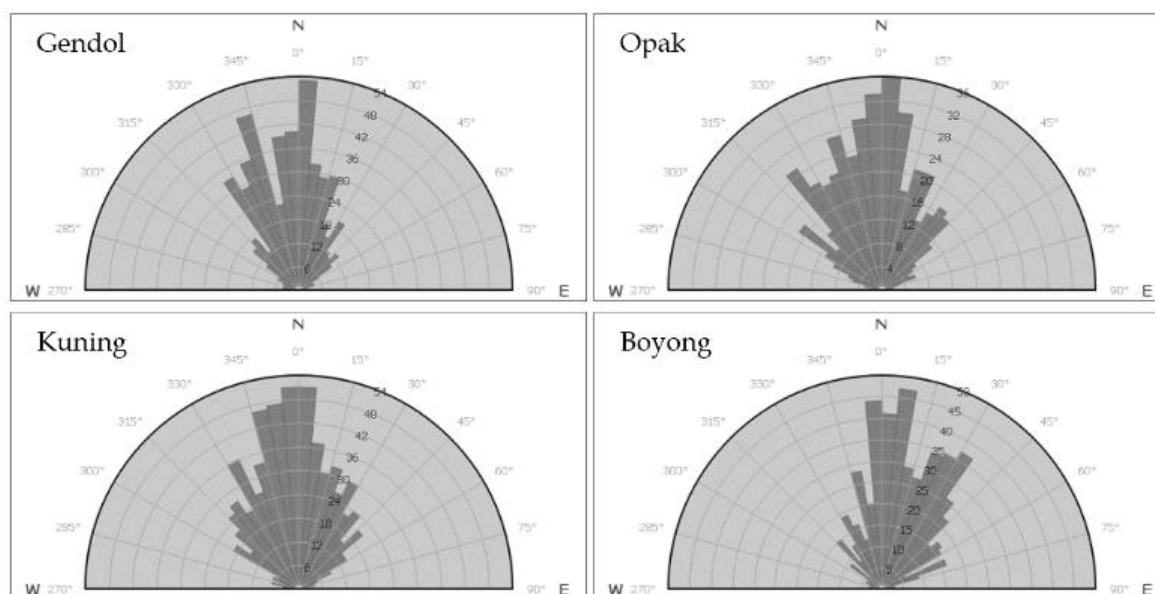


Figure 5. The lineament segmentation on the watershed of Gendol, Opak, Kuning, and Boyong

### 4.3 THE RATIO OF BIFURCATION (RB) AND DRAINAGE DENSITY (DD)

The ratio of bifurcation value is calculating on the tabulation of data based on watershed boundaries, and with values less than three or more than five indicates deformation has occurred (Verstappen, 1983). The results of calculations can see in the tabulation data obtained Rb value. Gendol River and downstream part of the River Opak, and Kuning River shows the value of deformation, while Boyong River does not show significant deformation. The Gendol River is a long concave shape with a higher Rb value indicating low peak flow discharge, and sediment deposition may occur longer. It can also indicate that there has been an erosion process due to the effects of the dominant geological structure. The Opak, Kuning, and Boyong rivers with relatively low Rb values indicate low surface flow. Few river channels produce sediment material with high

infiltration values and may indicate deeper groundwater flows.

Drainage density value or distribution value of the distribution of drainage density gets the reflection of different layers of volcanic rock (Strahler, 1957). The distribution of watershed flow assesses by knowing Rb and Dd's value to determine the deformed landform and lithological resistance. The lower Dd values are in the 3.44 Kuning River, and the Opak River 3.87 indicates a more resistant rock, found in lower reliefs being lightly eroded and having infiltration capacity with good permeability. The value of Dd in the Gendol River 4.55 can indicate the soft rocks. Boyong River with a Dd value of 4.76 shows a value twice as significant as Rb's value can indicate a strongly eroded watershed. The Gendol and Boyong rivers include a somewhat subtle texture classification, while the Opak and Yellow Rivers with medium texture (Table 3).

Table 3. The class's Rb value actively deformed on the Gendol River and downstream of the Opak and Kuning Rivers.

River	River Segment	Rb 1-2	Rb 2-3	Rb 3-4	Rb 4-5	Rb 5-6	Rb 6-7	Dd
Gendol	81	2.3	0.9	9.5				4.55
Opak	43	1.8	1.7	3.5				3.87
Kuning	68	1.7	1.8	1.3	4			3.44
Boyong	76	1.4	1.3	1.1	0.7	2.8	1.7	4.76

#### 4.4 THE SINUOSITY OF MOUNTAIN FRONT (SMF) AND VALLEY RATIO (VF)

The mountain's sinuosity is the analysis used from the variable value Smf can show the relationship between the form of land, geological structure, erosion rate, and tectonics. The balance between the erosion and lift strength can determine the value of the sinuosity or the end of the mountain face. The Smf value ranging from 1.2 to 1.6 is an active tectonic area with a full ridge shape indicating dominant swelling and erosion, the Smf value of 1.8-3.4 is the level of tectonic activity medium to low, and the Smf value of 2.0 - 5.0 represents the level of inactive tectonic activity (Doornkamp, 1986). Smf calculation uses topographic maps and imagery to calculate the mountain front

sinuosity, with 22 relief incisions. The analysis results show active tectonic activity classes and dominated classes of moderate tectonic activity. Valley ratio width to valley height ratio is the ratio index value that can reflect the level of lifting in an area (Keller & Pinter, 1996). Vf values can reflect the degree of maturity of a river valley (Bull & McFadden, 1977). A Vf value less than 0.5 has a high uplift rate, and a Vf ratio between 0.5 - 1 has a moderate uplift rate, and a Vf value greater than 1 has a low uplift rate. The calculation results show the value with low to high uplift level, with the value of the ratio of Vf top uplift level of 0.001 - 0.370, and with the value of the ratio Vf low uplift rate 1.207 - 15.293 (.).

Table 4). The Vf index uses to classify the difference between a valley and a cross-sectional shape of a river basin that resembles the letter U and has a high index value of Vf ratio, the value belonging to an area less affected by the tectonic activity. The valley with the shape of a river valley

that resembles the letter "V" has a low Vf value. That value belongs to the area of active tectonic activity. The analysis result with index Vf's value gets a value less than 0.5, equal to 65%, which counted from 22 incision relief. That value indicates that the River area domain by high elevation level.

Table 4. The mountain front (Smf) sinuosity determines the class of tectonic activity level and valley ratio index (Vf) to determine the uplift class.

No.	Smf	Tectonic	Vf	uplift
1	1.947	medium	4.290	low
2	1.363	active	0.021	high
3	1.594	active	0.034	high
4	1.957	medium	0.060	high
5	2.108	medium	2.284	low
6	1.826	medium	1.304	low
7	1.713	medium	1.847	low
8	2.013	medium	0.012	high
9	1.968	medium	0.092	high
10	1.823	medium	0.370	high
11	1.805	medium	11.607	very low
12	1.949	medium	1.207	low
13	1.824	medium	0.111	high
14	1.810	medium	0.046	high
15	1.635	medium	0.188	high
16	1.996	medium	0.047	high
17	2.087	medium	15.293	very low

18	1.715	medium	6.159	low
19	2.840	medium	0.036	high
20	1.928	medium	0.032	high
21	1.946	medium	0.001	high
22	2.510	medium	0.008	high

#### 4.5 ASYMMETRY FACTOR (AF)

Asymmetry factor obtained from comparing the river basin area with the total river basin area. AF analysis can classify the presence of tectonic activity in areas with weakly consolidated lithology of Quaternary. A stable AF state with a value of 50, whereas AF with values higher than 50 or less than 50 indicates river slope caused by tectonic activity (Keller & Pinter, 1996). The results of AF calculations in the Gendol River, Opak River, Yellow River, and Boyong River, each with a value of 32.0; 16.7; 31.9; and 19.4, a value <50, indicates a slope due to tectonic movement.

#### 4.6 STREAM LENGTH (SL)

The stream length value or high river gradient index derives from the multiplication of the river's total length by the ratio of the elevation difference from the point calculated by the river's length to the point calculated. The SL index measures river slope changes and evaluates the relationship between rock resistance, topography, and tectonic activity. High SL index values reflect river flow in hard rocks or areas with high activity levels. In contrast, low SL index values indicate low tectonic activity levels with less resistant lithology (Keller & Pinter, 1996). The value of SL obtained each value on the river flow 5.9; 12.2; 8.6; 8.8. In the similarly long-form river slopes, the Gendol River's calculations show a value (5.9) lower than that of other Rivers, reflecting the tectonic activity in the Gendol River lower than in the Opak River (12.2).

#### 4.7 HYPSONETRIC INTEGRAL (HI)

Hypsometric integrals are the equations for describing the shape of the hypsometric curve. Moreover, the distribution of elevation extending to a land area. From a single drain to all the land on Earth. The curve form from calculating the high proportion of the total basin (relative height) to the entire basin's total area

(related area). The shape of the hypsometric curve calculates by the hypsometric integral equation. Calculate to determine the erosion cycle with the stages of the young, mature, and old relief levels in a watershed (Keller & Pinter, 1996).

The hypsometric integral calculations showed the intermediate values and presented them on a sinusoidal shaped curve. Which indicates the development of the river is at an adult stage. Hypsometric data were obtained from DEM to assess and compare the morphological evolution of different forms of land. The shape of the curve and the integral can find information from a stream for erosion, tectonic activity, seasons, and lithologic factors. The results of the calculations and shown on the hypsometric curve show rivers with mature stadia. The mean value ( $\bar{x}$ ) calculated by comparison of elevation and river area (h/H and a/A). The integral value of Gendol River 0.407 and 0.480; the integral value of the Opak River 0.570 and 0.403; integral values on the Kuning River 0.403 and 0.487; and integral values of Boyong River 0.426 and 0.415. The value indicates that the integral equations of hypsometry are in the same river's progression

#### 4.8 TRANSVERSE TOPOGRAPHY SYMMETRY (T)

Transverse topography symmetry is the calculation used to detect the direction of the river's slope, and the value of T for a perfectly symmetric basin equals 0 ( $T = 0$ ). As the asymmetry value increases, the value of T will be close to the value of 1. This equation is calculated from the midline distance ratio of valleys to the maximum height (Da) with a diameter distance from the valley to the minimum height (Dd). Calculation of T value at Gendol River with value 0,48 until 0,94 with value  $x^{-0,65}$ ; on the Opak River with a value of 0.12 to 0.93 with a value of  $x^{-0.47}$ ; on the Kuning River with a value of 0.15 to 0.9 with the value of  $x^{-0.63}$ ; on Boyong River with a value of 0.23 to 0.91 with  $x^{-0.87}$ . The T value's accumulated calculation on the graph shows that the river's asymmetry

value has shifted from the left to the right and has moved towards the West.

#### 4.9 ELONGATION OF BASIN RATIO (EB)

Elongation of basin ratio or elongation ratio of river valley elongation shows the active form of land raised because of tectonic. The Eb value obtains from the ratio of the river basin's diameter divided by phi. With the length of the river basin. Eb may reflect longitudinal or circular basins and tectonic classification (Schumm, 1956). Based on the classification of river valley elongation (Chow, 1964), on various climate and geological conditions, the classification value ranges from; 0.6 for the elongated basin and active basin and 1.0 for tectonic, oval, and circular basins. Based on this standard classifies the river

basin as follows: circular (> 0.9), oval (0.8-0.9), less elongated (0.7-0.8), and elongated (<0.7). The low basin elongation ratio is an indicator of new tectonic activity (Bull & McFadden, 1977).

The values of rivers calculated from rivers above 0.002-0.004 indicate the elongate shape so that river characters classify as tectonically active. This parameter also shows the dominance of tectonic forces due to erosion. Based on the image analysis and topographic map calculation with a morphotectonic parameter with Rb, Dd, Hi, T, and Eb variables on Gendol River, Opak River, and Kuning River, and Boyong River. Asymmetry formed in the adult stage of stadia, in soft lithology to stern, and the state of the river has deformed, as it was knowing that there had been an elevation due to active tectonic activity.

Table 5. The morphotectonic table shows that the shape of each asymmetry river form in the mature stadia stage lies in soft to stiff lithology. The state river deformed, knowing that there had been an elevation due to active tectonic activity.

Parameter of Morphology	Gendol	Opak	Kuning	Boyong	Classification
Rb	4.3	2.4	2.2	1.5	Deformed
Dd	4.5	3.9	3.4	4.8	Soft – hard rock Lightly–strong eroded
Smf	1.4 – 2.8				Active tectonic
Vf	0.001 – 15.293				Uplift low-high
AF	32.0	16.7	31.9	19.4	Assymetri
SL	5.9	12.2	8.6	8.8	Active tectonic
Hi	h/H 0.4 a/A 0.5	h/H 0.6 a/A 0.4	h/H 0.4 a/A 0.5	h/H 0.4 a/A 0.4	Mature stadia
T	0.65	0.47	0.63	0.87	Asymmetri
Eb	0.004	0.003	0.003	0.003	Tectonic active

#### 5. CONCLUSIONS

- 1) The morphotectonic variable values with the GIS process from DEM data extraction from contour, aspect, slope, and hillshade forms show differences in deformation due to tectonic and non-deformation effects. The Opak River, Kuning River, and Boyong River are deformed, while the Gendol River is not deformed, with mature stadia classification.
- 2) Gendol River, Opak River, Kuning River, and Boyong River are analyzed and get the value that proves tectonic activity

involvement. Rb with value 4.3; 2.4; 2.2; 1.5 shows that the land has deformed. Dd with value 4.5; 3.9; 3.4; 4.8 shows soft rock density to hard, and erosion weak to moderate. Smf with values of 1.4 to 2.8 show active tectonics. A value of 0.001-15.293 shows a low to high uplift. AF with a value of each stream 32; 16.7; 31.9; 19.4 indicates river asymmetry. SL with a value of 5.9, 12.2; 8.6; 8.8 shows active tectonics. Hi with h/H values 0.4-0.6 a/A 0.4-0.5 the river on mature stadia. T value for each river with a value of 0.65; 0.47; 0.63; 0.87 shows the asymmetric river. Eb of each

river with a value of 0.003-0.003 shows the active tectonics.

- 3) The results of morphotectonic values indicate asymmetric rivers are flowing on rocks with rather stiff resistance. These values result in small depositions and medium active tectonic activity classes, with a high uplift rate, which indicates that the tectonic structure's movement still affects.
- 4) The result of lineament analysis shows that the geological structure is still active and continues until the topmost layer of volcanic deposits.

## REFERENCES

- Ahmed, F., Rao, K. 2016. Morphotectonic Studies of The Tuirini Drainage Basin; A Remote Sensing and Geographic Information System Perspective. *International Journal of Geology, Earth and Environment Science*, January-April, 6(1), pp. 54-65.
- Anfasha, A., Pranantya, P.A., Sukiyah, E. 2016. Characteristic of Morphometry dan Morphotectonic Cibeet Watershed, Selaawi Girijsaya Segment and Cikundul Watershed, Cibadak Majalaya Segment, Cianjur, West Java (in Indonesian). *Bulletin of Scientific Contribution*, 14(2), pp. 185-194.
- Bahrami, S. 2013. Tectonic controls on the morphometry of alluvial fans around Danekkhoshk anticline, Zagros, Iran. *Geomorphology*, Volume 180-181, pp. 217-230.
- Bali, B., Wani, A., Khan, R., Ahmad, S. 2016. Morphotectonic Analysis of the Madhumati Watershed, Northeast Kasmir Valley. *Saudi Society for Geosciences*, 9(390), pp. 1-17.
- Bull, W., McFadden, L.D. 1977. *Tectonic Geomorphology North and South of the Garlock Fault, California*. New York, State University New York, Birmingham, New York, pp. 115-138.
- Charbonnier, S. et al. 2013. Evaluation of the 2010 Pyroclastic Density Currents at Merapi Volcano From High-Resolution Satellite Imagery, Field Investigations, and Numerical Simulations. *Journal of Volcanology and Geothermal Research*, Volume 261, pp. 295-213.
- Chow, V. 1964. *Handbook of Applied Hydrology*. New York: McGraw Hill.
- Çöltekin, A. et al. 2016. Perceptual complexity of soil-landscape maps: a user evaluation of color organization in legend designs using eye-tracking. *International Journal of Digital Earth*, 14 10.pp. 1-22.
- Cox, R. T. 1994. Analysis of drainage-basin symmetry as a rapid technique to identify areas of possible Quaternary tilt-block tectonics: An example from the Mississippi Embayment. *The Geological Society of America Bulletin*, May, 106(5), pp. 571-581.
- Doornkamp, J.C. 1986. Geomorphological approaches to the study of neotectonics. *Journal of the Geological Society*, 143(2), pp. 335-342.
- Flores-Prieto, E. et al. 2015. Morphotectonic interpretation of the Makuyuni catchment in Northern Tanzania using DEM and SAR data. *Geomorphology*, Volume 248, pp. 427-439.
- Ganas, A., Pavlides, S., Karastathis, V. 2005. DEM-based morphometry of range-front escarpments in Attica, central Greece, and its relation to fault slip rates. *Geomorphology*, Volume 65, pp. 301-319.
- Geospatial, I.A. 2016. Geospatial of the Country (in Indonesian). [Online] Available at: <http://tanahair.indonesia.go.id/portal/landingpage> [Accessed 22 6 2017].
- Gertisser, R., Charbonnier, S.J., Keller, J., Quidelleur, X. 2012. The geological evolution of Merapi volcano, Central Java, Indonesia. *Bulletin of Volcanology*, 74(5), pp. 1213-1233.
- Helbig, C. et al. 2017. Challenges and strategies for the visual exploration of the complex. *International Journal of Digital Earth*, 13 May. pp. 1-7.
- Hunter, J., Brookinga, C., Reading, L., Vink, S. 2015. A web-based system enables the integration, analysis, and 3D sub-surface visualization of groundwater monitoring data and geological models. *International Journal of Digital Earth*, pp. 1-18.
- Jing, C., Shortridge, A., Lin, S., Wu, J. 2014. Comparison and validation of SRTM and ASTER GDEM for a subtropical landscape in Southeastern China. *International Journal of Digital Earth*, pp. 969-992.
- Kaplay, R., Babar, M., Mukherjee, S., Kumar, T. 2016. Morphotectonic Expression of Geological Structures in The Eastern Part of The South East Deccan Volcanic Province (around Nanded, Maharashtra, India). *Tectonics of the Deccan Large Igneous Province*.
- Keller, E., Pinter, N. 1996. *Active Tectonics. Earthquakes, Uplift, and Landscape*. 2nd ed. New Jersey: Upper Saddle River, N.J.: Prentice-Hall, c2002.
- McGuire, M.P., Roberge, M.C., Lian, J. 2016.

- Channeling the water data deluge: a system for flexible integration and analysis of hydrologic data. *International Journal of Digital Earth*, 19 3.pp. 272-299.
- Molin, P., Pazzaglia, F., Dramis, F. 2004. Geomorphic expression of active tectonics in rapidly-deforming forearc, Sila Massif, Calabria, Southern Italy. *American Journal of Science*, pp. 559-589.
- Moore, I.D., Grayson, R.B., Ladson, A.R. 1991. Digital Terrain Modelling: A Review of Hydrological, Geomorphological, and Biological Applications. *Hydrological Processes*, 6 September, Volume 5, pp. 3-30.
- Napieralski, J., Barr, I., Kamp, U., Kervyn, M. 2013. Remote Sensing and GIScience in Geomorphological Mapping. *Treatise on Geomorphology*, Volume 3, pp. 187-227.
- Omar M.A. Radaideh, B. G. R. M. J. M. 2016. Detection and analysis of morphotectonic features utilizing satellite remote sensing and GIS: An example in SWJordan. *Geomorphology*, Volume 275, pp. 58-79.
- Paripurno, E.T. 2009. Characteristic of Volcanic Lava Flow as Response to Different Types of Eruption Since Holosen. Bandung: Doctoral Program of Padjadjaran Universitas (dissertation).
- Petrik, A., Jordan, G. 2017. Systematic Digital Terrain Model Construction And Model Verification With Multi-Source Field Data. *Morphotectonic Analysis In The Villany Hills and Its Surroundings, SW Hungary. Carpathian Journal of Earth and Environmental Sciences*, 12(1), pp. 217-224.
- Pike, R. J., Wilson, S.E. 1971. Elevation-relief ratio, hypsometric integral, and geomorphic area-altitude analysis. *Bulletin of the Geological Society of America*, 82(4), pp. 1079-1084.
- Schumm, S.A. 1956. Evolution of drainage system and slope badlands at Perth Amboy, New Jersey. *Geological Society of America Bulletin*, May, 67(5), pp. 597-646.
- Sharma, G., Ray, P.C., Mohanty, S. 2017. Morphotectonic analysis and GNSS observations for assessing relative tectonic activity in the Alakhanda basin of Garhwal Himalaya, India. *Geomorphology*, Volume 301, pp. 108-120.
- Shi, X., Xue, B. 2016. Deriving a minimum set of viewpoints for maximum coverage over any given digital elevation model data. *International Journal of Digital Earth*, 20 7.pp. 1-15.
- Strahler, A. 1957. *Quantitative Analysis of Watershed Geomorphology*. Transactions, American Geophysical Union, pp. 913-920.
- Sukiyah, E. 2017. *Geographic Information System: Concepts and Applications in Quantitative Analysis (in Indonesian)*. 1 ed. Bandung(West Java): Unpad Press.
- Sukiyah, E. et al. 2015. Morphotectonic and Satellite Imagery Analysis For Identifying Quarternary Fault At Southern Part Of Cianjur-Garut Region, West Java, Indonesia. Bandung, Asian Association on Remote Sensing.
- Szekely, B., Karátson, D. 2004. DEM-based morphometry as a tool for reconstructing primary volcanic landforms: examples from the Börzsony Mountains, Hungary. *Geomorphology*, Volume 63, pp. 25-37.
- Van Bemmelen, R. 1949. *The Geology of Indonesia*. Netherlands: Government Printing Office, The Hague.
- Verstappen, H.T. 1983. *Applied Geomorphology: Geomorphological Surveys for Environmental Development*. New York: Elsevier Science Pub. Co. Inc.
- Wolosiewicz, B. 2016. Morphotectonic control of the Bialka drainage basin (Central Carpathians): Insights from DEM and Morphometric Analysis. *Contemp. Trends. Geosci*, 5(1), pp. 61-82.
- Yasin, A.M., Sukiyah, E., Sulaksana, N., Isnaniawardhani, V. 2016. Morphotectonic Phenomenon of SRTM Imagery in Kendari Bay Area. *Bulletin of Scientific Contribution*, 14(2), pp. 163-170.